Decreased Opacity without Cystic Airspace

13

Mosaic Attenuation

Definition

Mosaic attenuation pattern appears as patchwork of regions of differing attenuation that may represent (a) patchy interstitial disease, (b) obliterative small airway disease, or (c) occlusive vascular disease [1, 2]. Mosaic attenuation pattern caused by the latter two disease categories is called mosaic perfusion (Figs. 13.1 and 13.2). The combination of mixed lung attenuations (combination of ground-glass opacity, normal lung, and reduced lung attenuation as a result of mosaic perfusion) often gives the lung a geographic appearance and has been termed the *head-cheese sign*.

Diseases Causing the Mosaic Attenuation Pattern

Causes of mosaic attenuation pattern include infiltrative lung disease, airway disease, and vascular disease. Mosaic attenuation can be seen in a variety of airway diseases including bronchiectasis, *cystic fibrosis* (Fig. 13.2), allergic bronchopulmonary aspergillosis (ABPA), asthma, and *constrictive bronchiolitis* (Fig. 13.1). Vascular causes of mosaic perfusion include *chronic pulmonary thromboembolism* (Fig. 13.3) and *pulmonary arterial hypertension* (Fig. 13.4) (Table 13.1). Various interstitial lung diseases characterized by patchy areas of ground-glass opacity (GGO) are also the causes of mosaic attenuation pattern. Please note Chaps. 20 and 21 areas of GGO with or without reticulation. Mixed infiltrative and obstructive diseases (hypersensitive pneumonitis, sarcoidosis, atypical infection with associated bronchiolitis) also cause mosaic attenuation pattern.

Distribution

In cystic fibrosis, proximal or perihilar bronchi are always involved when bronchiectasis is present. All lobes are typically involved, although early in the disease, abnormalities show often predominantly upper lobe predominance in their distribution [3]. Although there are some overlaps, areas of mosaic perfusion in cystic fibrosis correspond to pulmonary lobules or subsegments [4], whereas those in chronic thromboembolism are typically segmental or subsegmental in distribution [5]. In subacute hypersensitivity pneumonitis, areas of GGO are usually diffuse, bilateral, and symmetric. However, areas of mosaic perfusion are multifocal and usually have a configuration consistent with involvement of single or multiple adjacent pulmonary lobules [6].

Clinical Considerations

Cystic fibrosis results from an autosomal-recessive genetic defect in the structure of the cystic fibrosis transmembrane regulator protein, which leads to abnormal chloride transport across epithelial membranes [7]. ABPA results from both type I and type III hypersensitivity reactions to the endobronchial growth of Aspergillus species and is characteristically associated with eosinophilia, symptoms of asthma, and typical imaging findings [8]. Conditions associated with constrictive bronchiolitis include heart–lung or lung transplantation, chronic allograft rejection, allogeneic bone marrow transplantation with chronic graft-versus-host disease, and collagen vascular disease, especially rheumatoid arthritis [9]. Pulmonary arterial hypertension may be idiopathic or arise in association with chronic pulmonary thromboembolism; pulmonary embolism caused by tumor cells, parasitic material, or foreign material; parenchymal lung disease; liver disease; vasculitis; human immunodeficiency virus infection; or a left-to-right cardiac shunt [5]. Most cases of hypersensitivity pneumonitis develop only after many years of inhaling allergens, which include microbes, animal or plant proteins, and certain chemicals [10].

K.S. Lee et al., *Radiology Illustrated: Chest Radiology*, Radiology Illustrated,
DOI 10.1007/978-3-642-37096-0_13, © Springer-Verlag Berlin Heidelberg 2014

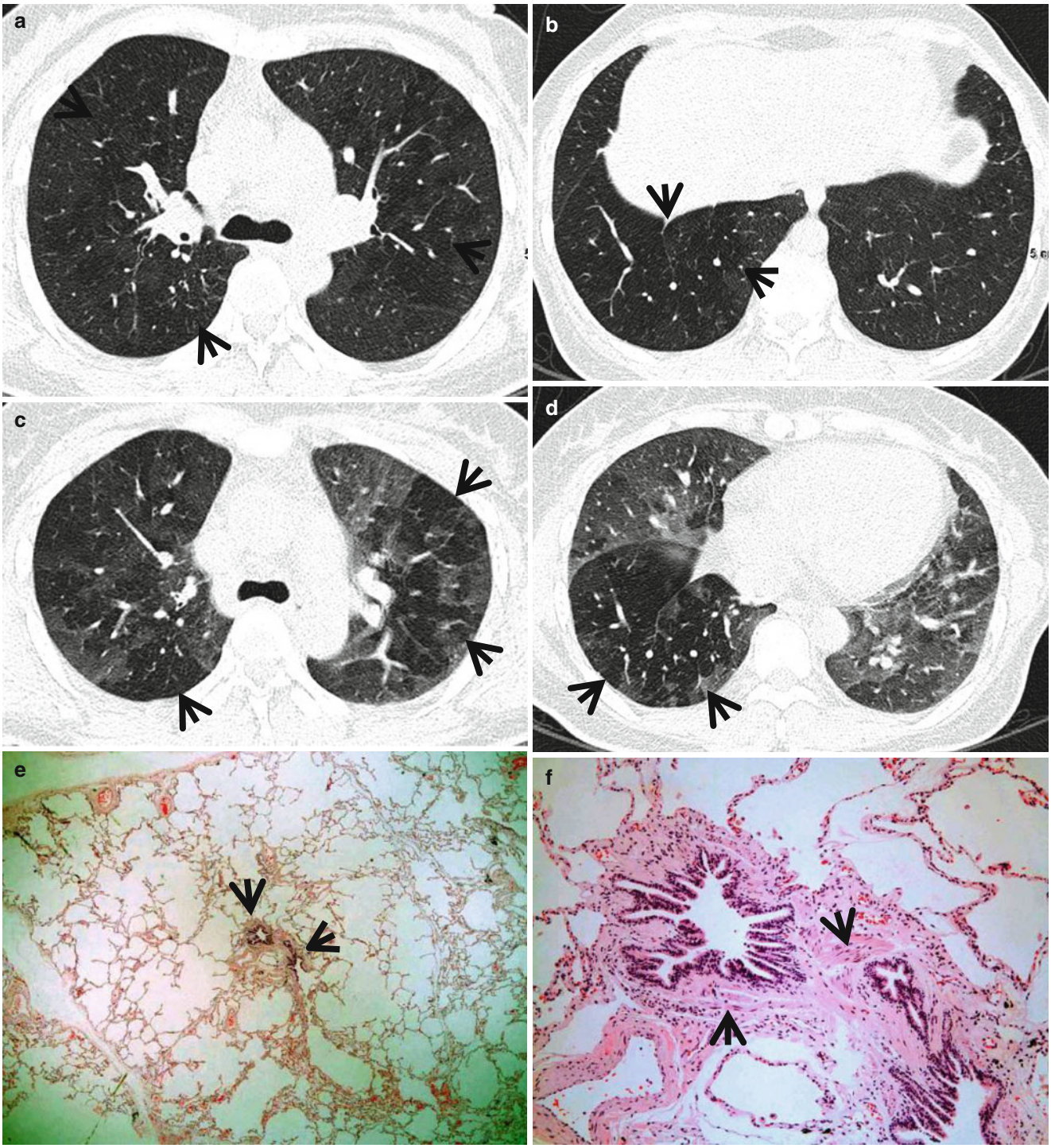

Fig. 13.1 Constrictive bronchiolitis in a 45-year-old woman. (**a**, **b**) Lung window images of thin-section (1.5-mm section thickness) CT scans obtained at levels of main bronchi (**a**) and liver dome (**b**), respectively, show patchy areas of mosaic perfusion (*arrows*) in both lungs. (**c**, **d**) Expiratory CT scans obtained at similar levels to (**a**, **c**) and (**b**, **d**), respectively, demonstrate air trapping (*arrows*) more clearly in both lungs. (**e**) Low-magnification (×40) photomicrograph of pathologic specimen obtained with surgical lung biopsy displays bronchiolar collagen-type fibrosis inducing luminal narrowing (*arrows*) of a membranous bronchiole. (**f**) High-magnification photomicrograph (×200) discloses fibrous thickening of lamina propria between epithelium and muscularis mucosa (*arrows*)

Key Points for Differential Diagnosis

1. Regardless of its cause, when mosaic perfusion is present, pulmonary vessels in the areas of decreased opacity often appear smaller than vessels in relatively dense areas of the lung [11, 12]. This discrepancy can be quite helpful in distinguishing mosaic perfusion from patchy appearance of GGO. In patients with GGO, vessels usually appear equal in size throughout the lungs.
2. In patients with mosaic perfusion resulting from airway diseases, abnormally dilated or thick-walled airways may be visible in the relatively lucent lung regions [2], and lobular areas of low attenuation are common [13]. Air trapping on expiratory scans is often helpful in confirming the diagnosis. Attenuation differences are accentuated scans obtained on expiration [14].
3. In patients with mosaic perfusion resulting from vascular diseases, areas of low attenuation are usually larger than lobules. In patients with mosaic perfusion occurring in association with chronic pulmonary embolism or pulmonary arterial hypertension, enlargement of the main pulmonary arteries may be visible.

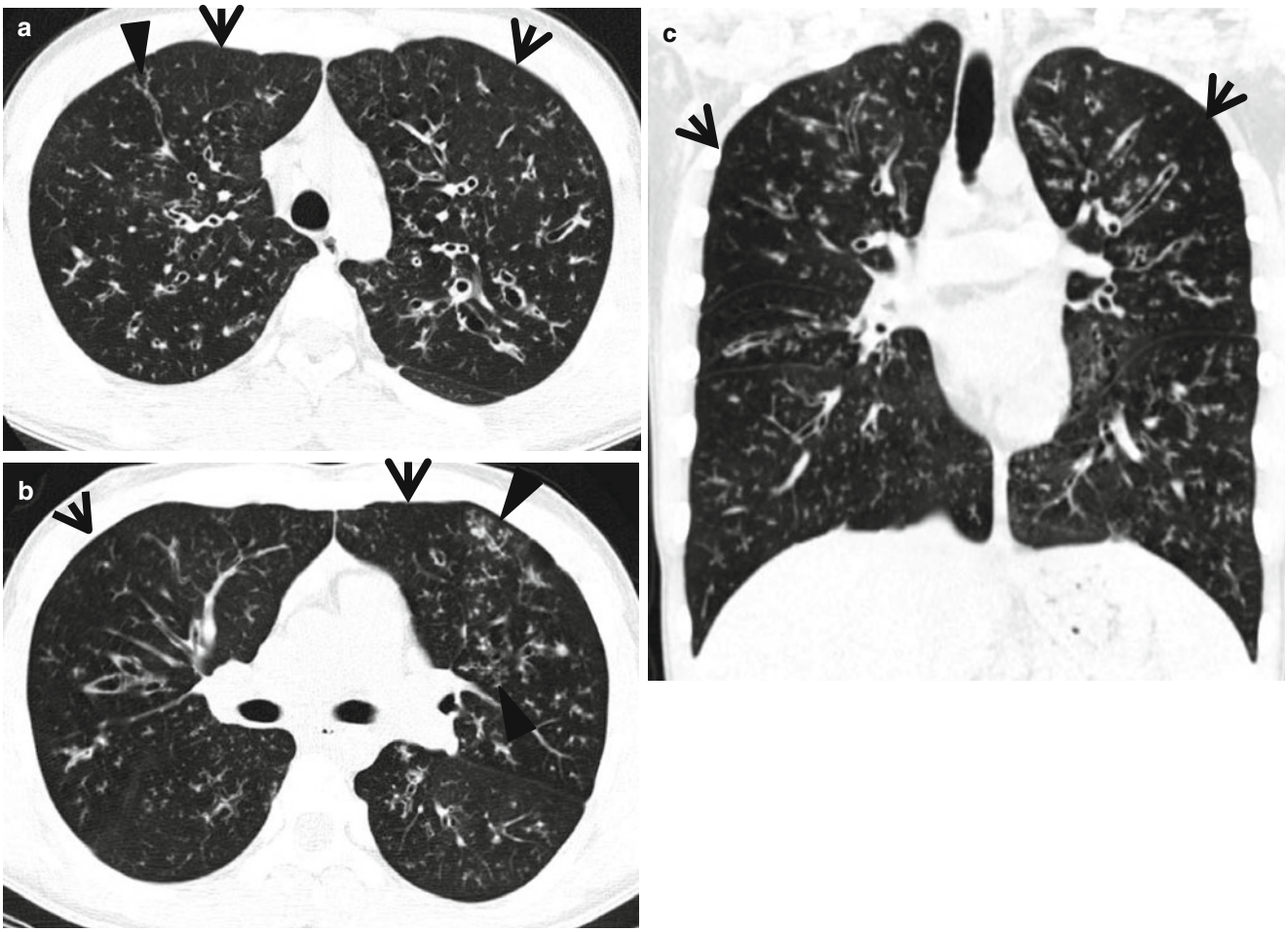

Fig. 13.2 Cystic fibrosis in a 24-year-old man who underwent lung transplantation. (**a**, **b**) Lung window images of thin-section (2.5-mm section thickness) CT scans obtained at levels of aortic arch (**a**) and main bronchi (**b**), respectively, show extensive areas of bronchiectasis and cellular bronchiolitis (*arrowheads*) in both lungs. Also note bilateral patchy areas of mosaic attenuation (*arrows*). (**c**) Coronal reformatted CT image (2.0-mm section thickness) demonstrates bronchiectasis and cellular bronchiolitis in both lungs. Also note patchy areas of mosaic attenuation (*arrows*), in which oligemia (decreased caliber of vessels) findings are clearly visualized. (**d**) Gross pathology and photomicrographs at corresponding area indicated by bars of explanted lungs disclose pus in bronchiectatic or bronchiolectatic airways. In a portion of right lung, airway wall fibrosis and resultant postobstructive airway dilatation are seen (*open arrows*)

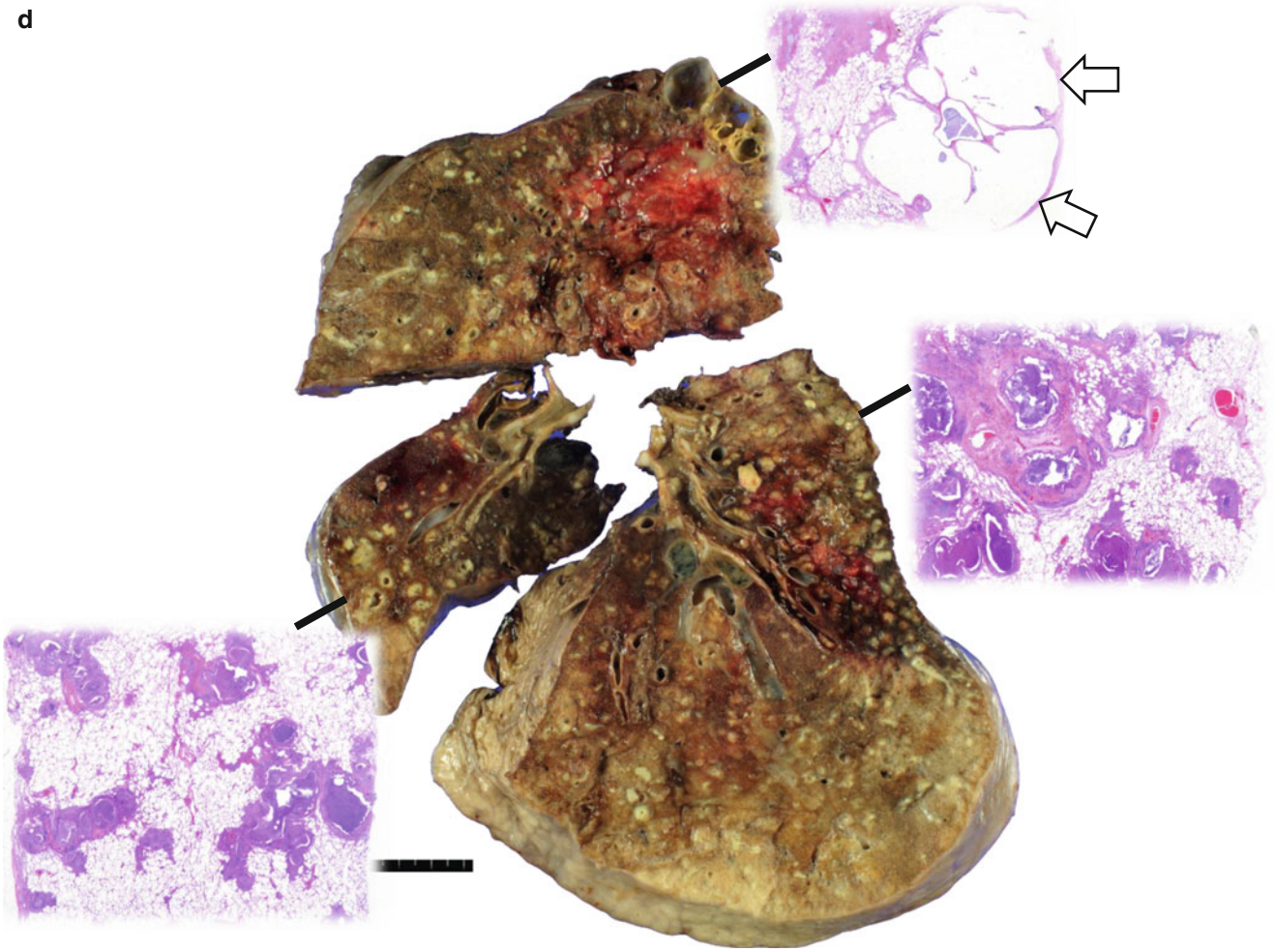

Fig. 13.2 (continued)

4. Characteristic CT vascular signs including webs or bands, intimal irregularities, abrupt narrowing, or complete obstruction of the pulmonary arteries with enlarged main pulmonary arteries enable the diagnosis of chronic pulmonary thromboembolism in patients with mosaic perfusion [15].
5. Data from electrocardiographically (ECG)-gated multidetector CT studies show that functional parameters such as right pulmonary artery distensibility, systolic–diastolic right ventricular outflow tract dimensions, and diastolic wall thickness can be measured with good interobserver agreement and used as reliable criteria for a diagnosis of pulmonary hypertension [16]. Mosaic lung perfusion is found significantly more often among those with pulmonary arterial hypertension due to vascular disease than among those with pulmonary arterial hypertension due to cardiac or lung disease (74 % [17 of 23] vs. 8 % [3 of 38] of the patients in one series) [17].
6. The head-cheese sign is usually indicative of mixed infiltrative and obstructive disease, usually associated with bronchiolitis. In patients with this appearance, the presence of GGO is caused by lung infiltration, whereas the presence of mosaic perfusion with decreased vessels sign is usually caused by small airway disease. The combination of GGO on inspiratory scans and air trapping on expiratory scans is considered indicative of a mixed infiltrative and obstructive disease such as hypersensitivity pneumonitis [14].

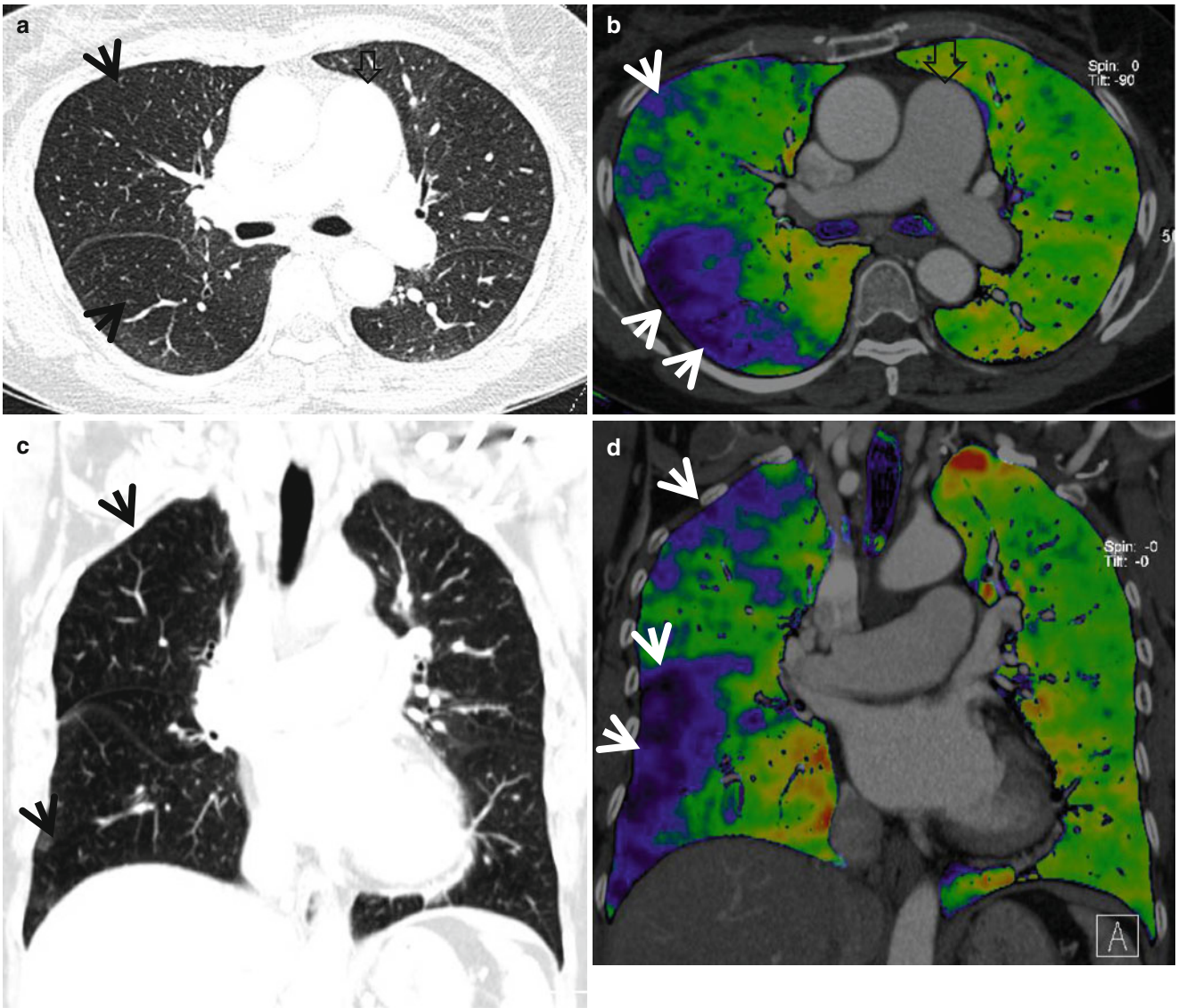

Fig. 13.3 Mosaic perfusion in a 58-year-old woman with chronic thromboembolism and pulmonary arterial hypertension. (**a**) Lung window image of CT scan (1.0-mm section thickness) obtained at level of main bronchi shows mosaic attenuation areas (*arrows*) in right lung. Also note markedly enlarged main pulmonary artery. (**b**) Iodine perfusion map obtained with dual-source dual-energy CT clearly demonstrates areas of mosaic perfusion (*arrows*, *blue-colored areas*). (**c**) Coronal reformatted image (2.0-mm section thickness) shows multifocal areas (*arrows*) of mosaic attenuation. (**d**) Iodine perfusion map depicts more clearly mosaic perfusion areas (*arrows*)

Cystic Fibrosis

Pathology and Pathogenesis

Cystic fibrosis is an autosomal-recessive disease with a mutation of cystic fibrosis transmembrane conductance regulator (CFTR) gene and multisystem involvement. Patients have abnormal transport of chloride and sodium across the respiratory epithelium, resulting in thickened airway secretions and susceptibility to recurrent infections. Grossly, widespread bronchiectasis (more severe in upper lobe) with thick mucus plugs, pleural fibrosis or adhesions, pneumonic consolidation, and lobar atelectasis are seen in an end-stage disease (Fig. 13.2). Microscopically, acute and chronic inflammations involving the large and small airways associated with bronchial gland and goblet cell hyperplasia, squamous metaplasia, and mucostasis are frequently seen (Fig. 13.2).

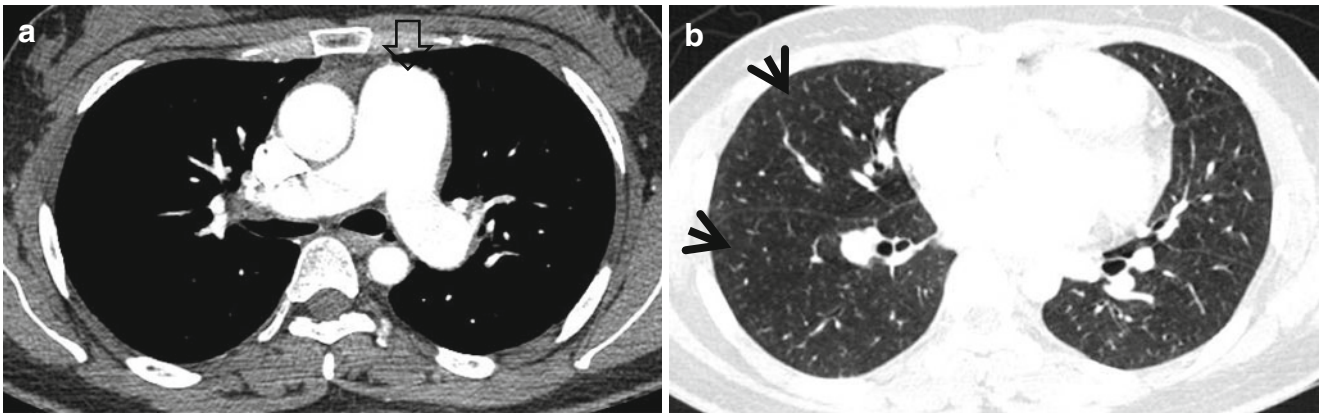

Fig. 13.4 Mosaic perfusion in a 28-year-old woman with idiopathic pulmonary arterial hypertension. (**a**) Mediastinal window image of enhanced CT (1.0-mm section thickness) scan obtained at level of main bronchi shows markedly enlarged main pulmonary artery (*open arrow*). (**b**) Lung window image obtained at level of right inferior pulmonary vein demonstrates suspicious areas of mosaic attenuation (*arrows*)

Table 13.1 Common diseases manifesting as mosaic attenuation

Disease	Key points for differential diagnosis
Airway disease	
Bronchiectasis	Bronchial dilatation with peribronchial thickening, signet ring sign
Cystic fibrosis	Mosaic perfusion, bronchiectasis involving upper lobes
ABPA	Central bronchiectasis with high-attenuation mucus plugging, mosaic perfusion
Asthma	Thickening and narrowing of the medium-sized and small bronchi, cylindrical bronchiectasis, centrilobular nodules, multifocal and patchy areas of mosaic perfusion
Constrictive bronchiolitis	Mosaic perfusion, air trapping on expiratory scans
Vascular disease	
Chronic pulmonary thromboembolism	Mosaic perfusion, ipsilateral airway dilatation, vascular findings of chronic embolism
Pulmonary arterial hypertension	Mosaic perfusion, central pulmonary arterial dilatation in the absence of detectable intraluminal thrombi
Mixed infiltrative and obstructive disease	
Subacute hypersensitivity pneumonitis	Combination of GGO on inspiratory scan and air trapping on expiratory scan
Sarcoidosis	Associated with perilymphatic micronodules
Atypical pneumonia with bronchiolitis	Patchy areas of GGO and centrilobular nodules, mosaic perfusion

Note: *ABPA* allergic bronchopulmonary aspergillosis, *GGO* ground-glass opacity

Symptoms and Signs

Since cystic fibrosis is a genetic disease resulting in complications in multiple organs, especially involving the lungs and pancreas, it mimics a number of other diseases. Usual respiratory presentations in adults include cough, sputum, wheezing, dyspnea, recurrent respiratory tract infection, and cor pulmonale if advanced. Usual gastrointestinal presentations in adults are recurrent abdominal pain, biliary cirrhosis with portal hypertension, and recurrent pancreatitis. Infertility may occur.

CT Findings

The predominant HRCT finding in early stage of cystic fibrosis is a mosaic perfusion due to air trapping related to small airway disease. Other typical CT features include bronchiectasis and peribronchial thickening, mainly involving the upper lobes, and centrilobular nodules or a tree-in-bud pattern and atelectasis or consolidation secondary to mucous plugging [3, 18] (Fig. 13.2). Bronchiectasis is most often cylindrical, but varicose and cystic bronchiectasis can be seen in advanced cases.

CT–Pathology Comparisons

Cystic fibrosis causes abnormal mucous gland secretions and the subsequent effect of inflammation and infection on airways [3]. The earliest and most universal pathologic lesion of cystic fibrosis is mucous obstruction of bronchioles and small bronchi (Fig. 13.2). A mosaic perfusion, which is the predominant early HRCT findings of cystic fibrosis, is caused by air trapping related to mucous obstruction and inflammation of bronchioles and small bronchi (Fig. 13.2). The elicited inflammatory response damages the normal structure of the airways, and bronchiectasis develops. Upper lobe predominance of bronchiectasis and peribronchial thickening may reflect an effect of gravity on the elastin-damaged parenchymal tissue. Obstruction of airways by mucous plugs results in centrilobular small nodules or a tree-in-bud pattern and atelectasis or consolidation on HRCT.

Patient Prognosis

Treatment consists of control of mucus retention and chronic infection in the lungs, replacement of pancreatic enzymes, and nutritional therapy. New therapeutic approaches, including pharmacologic interventions and gene transfer, offer hope for further advances [19]. Lung transplantation has become an accepted therapy for respiratory failure secondary to cystic fibrosis. The outcome is highly variable, but 50 % of patients can now be expected to survive beyond 37 years.

Constrictive Bronchiolitis

Pathology and Pathogenesis

Constrictive bronchiolitis is a small airway disease in which variable narrowing or obliteration of airway lumens occurs. Histologically, the disease shows submucosal scarring, concentric luminal narrowing, adventitial scarring, and chronic inflammation. In the late stage, the lumen is completely occluded by the fibrosis (Fig. 13.1).

Symptoms and Signs

Clinically, constrictive bronchiolitis is characterized by progressive airflow obstruction with poor responsiveness to medical therapy and high mortality rates [20]. Patients complain of cough and dyspnea, which progress relentlessly over weeks to months. Physical examination reveals inspiratory squeaks in 40–60 % of patients.

CT Findings

The main HRCT findings usually consist of areas of mosaic perfusion associated with vessels of decreased caliber on inspiratory scans and air trapping on expiratory scans [21]. Air trapping on expiratory HRCT is the most sensitive sign to detect constrictive bronchiolitis on HRCT [22] (Fig. 13.1). Central and peripheral bronchiectasis is also commonly present. Other findings include centrilobular small nodules and tree-in-bud patterns.

CT–Pathology Comparisons

Mosaic perfusion on HRCT is presumably caused by hypoventilation of the alveoli distal to the bronchial obstruction, which leads to secondary vasoconstriction. This vasoconstriction can be seen on CT scans as areas of decreased attenuation [23] (Fig. 13.1). Bronchiectasis may be secondary to the constrictive bronchiolitis itself or to a prior insult to the bronchial wall. Centrilobular small nodules and tree-in-bud patterns on HRCT are caused by peribronchiolar thickening and bronchiolectasis with secretions [24].

Patient Prognosis

Prognosis of constrictive bronchiolitis, irrespective of etiology, is poor. Most patients progressively deteriorate and are ultimately fatal due to respiratory failure within months to years. Macrolide antibiotics exhibit immunomodulatory effects and have been used.

Chronic Pulmonary Thromboembolism

Pathology and Pathogenesis

Chronic pulmonary thromboembolism (PE) causes pulmonary hypertension secondary to obstruction of arteries due to organized thrombi. In the lung of chronic PE, distended capillaries, multifocal microscopic foci of alveolar wall necrosis with focal inflammation, small amount of fibrinous exudate, and edema fluid can be seen. Variable amount of bronchopneumonia may be accompanied.

Symptoms and Signs

Patients with chronic PE typically present with nonspecific symptoms occurring in those with other causes of pulmonary

hypertension [25]. The symptoms include progressive dyspnea on exertion, chronic fatigue, chest discomfort, palpitations, or syncope. Cardiac murmur may be heard. Lower extremity edema, ascites, hepatomegaly, and cyanosis can be found.

CT Findings

The most common pulmonary parenchymal finding of chronic PE is a mosaic perfusion pattern (combination of areas of decreased attenuation and perfusion adjacent to areas of increased attenuation and perfusion) [15] (Fig. 13.3). Mosaic perfusion patterns are typically distributed in segmental and subsegmental patterns [26]. Chronic PE may also be associated with ipsilateral airway dilatation [27]. Vascular findings of chronic PE include webs or bands, intimal irregularities, abrupt narrowing or complete obstruction of pulmonary arteries, and enlargement of main pulmonary artery [15].

CT–Pathology Comparisons

The areas of decreased attenuation and vascularity on HRCT correspond to the lung distal to partially or completely occluded vessels, whereas the areas of increased attenuation and vascularity are the result of blood flow redistribution to the normal lung. It has been postulated that airway dilatation is secondary to retraction of fibrous tissue within the vascular lumen [27].

Patient Prognosis

Historical data indicate that chronic PE, if left untreated, is associated with a poor 5-year survival, ranging from 10 to 40 % [25]. Patients should receive lifelong anticoagulation therapy. Pulmonary thromboendarterectomy is the procedure of choice in symptomatic patients with chronic PE. The overall perioperative mortality rates at experienced centers range from 4 to 7 %. Pulmonary thromboendarterectomy has improved the 6-year survival rate up to 75 %.

Idiopathic Pulmonary Arterial Hypertension

Pathology and Pathogenesis

Medial hypertrophy and concentric or eccentric intimal fibrosis of the pulmonary arteries (muscular arteries) are seen in all forms of pulmonary hypertension [28].

Symptoms and Signs

The most common presenting symptom in patients with pulmonary arterial hypertension is dyspnea on exertion [29]. Other common complaints include fatigue, lack of energy, chest pain, syncope, palpitations, and lower extremity edema. On auscultation, an accentuated pulmonic component of S2 is present in most patients with pulmonary arterial hypertension.

CT Findings

Characteristic vascular features of idiopathic pulmonary arterial hypertension on CT are central pulmonary artery dilatation, usually in the absence of detectable intraluminal thrombi, small tortuous peripheral vessels representing plexogenic arteriopathy, and an abrupt decrease in the caliber of segmental and subsegmental arteries [5]. Additional CT findings include right heart enlargement, pericardial effusion, and mosaic perfusion pattern in lung parenchyma (Fig. 13.4). Mosaic perfusion pattern in idiopathic pulmonary arterial hypertension is characterized by focal perivascular hyper-attenuating areas in a peripheral or perihilar distribution or small, scattered, well-defined areas of low attenuation corresponding to the anatomic unit of a secondary pulmonary lobule with adjacent areas of increased attenuation in a patchy and diffuse distribution [30]. Dilatation of bronchial and nonbronchial systemic arteries is less commonly seen than in pulmonary hypertension due to chronic PE.

CT–Pathology Comparisons

Central pulmonary artery enlargement on CT is associated with wall thickening of elastic and large muscular arteries along with their luminal dilatation. Thickening is predominantly the result of intimal fibrosis in the larger vessels and a combination of intimal fibrosis and medial muscle hypertrophy and hyperplasia in the smaller muscular branches. In large dilated vessels, atherosclerotic plaques, sometimes complicated by calcification, also may be seen.

The plexogenic pulmonary arteriopathy is seen in the muscular pulmonary arteries, most characteristic of which is a plexiform lesion referring to localized focus of vascular dilatation associated with an intraluminal plexus of slit-like vascular channels separated by a variable number of fibroblast-like cells. The lesion is noted in a short distance beyond the origin of a small supernumerary branch (usually 100–200 um in diameter). Additional pathology in plexogenic arteriopathy is the presence of arterial intimal fibrous tissue with a solid appearance and being distributed in a

more or less concentric fashion in the vessel lumen. Occasionally, the intimal fibrosis is eccentric in location or traverses the lumen. The plexogenic arteriopathy is thought to be related to the vascular pruning (central arterial enlargement, peripheral vascular obliteration, and mosaic perfusion).

Patient Prognosis

With advances in knowledge of the disease and the availability of newer therapeutic agents, such as endothelin receptor antagonists, phosphodiesterase inhibitors, and prostanoids, survival of patients with idiopathic pulmonary arterial hypertension has improved but still remains suboptimal. The French Registry demonstrated that 1-, 2-, and 3-year survivals of pulmonary arterial hypertension are 85.7, 69.5, and 54.9 % for incident cases, respectively [31].

Airway Disease (Bronchiectasis and Bronchiolectasis)

Definition

Bronchiectasis is irreversible localized or diffuse bronchial dilatation, usually resulting from chronic infection, proximal airway obstruction, or congenital bronchial abnormality [1, 32] (Fig. 13.5). Morphologic criteria on thin-section CT scans include bronchial dilatation with respect to the accompanying pulmonary artery (signet ring sign), lack of tapering of bronchi, and identification of bronchi within 1 cm of the pleural surface [33] (Fig. 13.5). Bronchiectasis may be classified as cylindric, varicose, or cystic, depending on the appearance of the affected bronchi. It is often accompanied by bronchial wall thickening, mucoid impaction (please note Chap. 10), and small airway abnormalities [33].

Bronchiolectasis is defined as dilatation of bronchioles. When dilated bronchioles are filled with exudates and are thick walled, they are visible as a tree-in-bud pattern or as centrilobular nodules on CT [34].

Traction bronchiectasis and bronchiolectasis, respectively, represent irregular bronchial and bronchiolar dilatation caused by surrounding retractile pulmonary fibrosis [35].

Diseases Causing the Bronchiectasis and Bronchiolectasis

Bronchiectasis can result from chronic or severe bacterial infection (*Staphylococcus*, *Klebsiella*, *Mycobacterium tuberculosis*, nontuberculous mycobacterial disease), fungal (histoplasmosis) infection, and viral (Swyer-James-MacLeod syndrome, HIV infection) infection (Fig. 13.6). Bronchiectasis may occur in association with a variety of genetic abnormalities, especially those with abnormal mucociliary clearance, immune deficiency, or structural abnormalities of the bronchus or bronchial wall (cystic fibrosis, alpha-1-antitrypsin deficiency, *dyskinetic cilia syndrome* (Fig. 13.7), Williams–Campbell syndrome, Mounier–Kuhn syndrome, immunodeficiency syndromes). Noninfectious causes of bronchiectasis include allergic bronchopulmonary aspergillosis (ABPA); asthma, bronchial obstruction by tumor, foreign body, or congenital abnormalities; and systemic diseases (collagen vascular disease and inflammatory bowel disease). Bronchiectasis may also occur in patients with constrictive bronchiolitis including chronic graft-versus-host disease (Table 13.2). Bronchiolectasis is usually associated with bronchiolitis (please refer to section "Small Nodules with Centrilobular Distribution" in Chap. 18). In patients with lung fibrosis (usual interstitial pneumonia, nonspecific interstitial pneumonia) and distortion of lung architecture (pulmonary tuberculosis), traction bronchiectasis and bronchiolectasis are commonly present.

Distribution

Bronchiectasis as sequelae of pulmonary tuberculosis typically involves upper lobes [36]. In nodular bronchiectatic form of nontuberculous mycobacterial disease, bronchiectasis usually involves the right middle lobe, lingular division of the left upper lobe, and both lower lobes. In cystic fibrosis, proximal or perihilar bronchia are always involved when bronchiectasis is present. All lobes are typically involved, although early in the disease, abnormalities show often predominantly upper lobe predominance in their distribution [3]. Although central or diffuse bilateral bronchiectasis is common in patients with dyskinetic cilia syndrome, bronchiectasis involves predominantly or exclusively the lower lobes [37]. In Williams–Campbell syndrome, varicose and cystic bronchiectases are limited to the fourth-, fifth-, and sixth-generation bronchi [38]. ABPA typically involves segmental and subsegmental bronchi of the upper lobes.

Clinical Considerations

Cystic fibrosis results from an autosomal-recessive genetic defect in the structure of the cystic fibrosis transmembrane regulator protein, which leads to abnormal chloride transport across epithelial membranes [7]. The major clinical manifestations of cystic fibrosis are obstructive pulmonary disease and pancreatic insufficiency. Dyskinetic cilia syndrome is a group of autosomal-recessive disorders associated with defective ciliary structure and function and

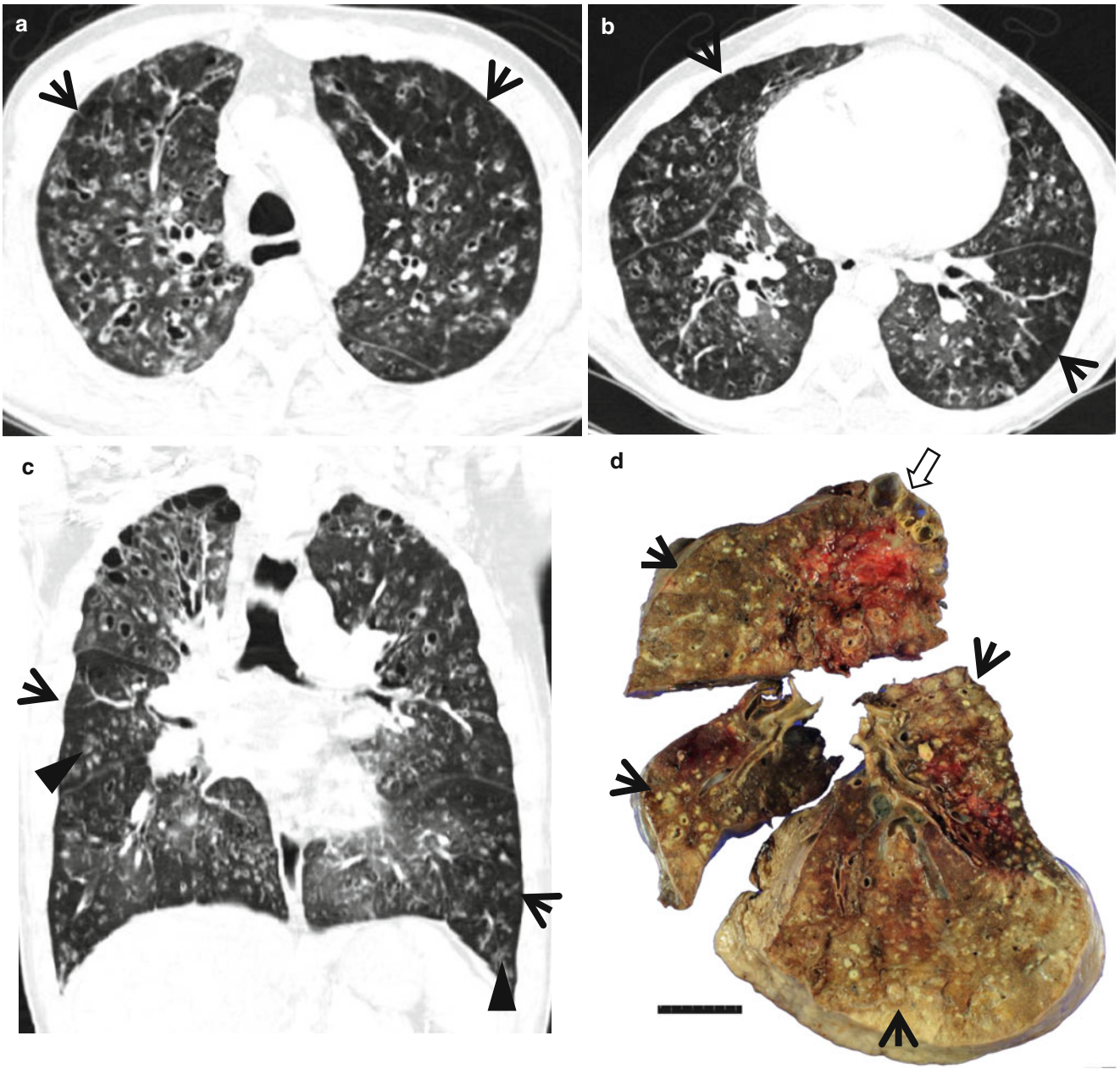

Fig. 13.5 Extensive bronchiectasis in both lungs in a 44-year-old man in whom specific causes for bronchiectasis could not be elucidated. Patient received bilateral lung transplantation. (**a**, **b**) Lung window images of CT scans (2.5-mm section thickness) obtained at levels of aortic arch (**a**) and basal segmental bronchi (**b**), respectively, show extensive bronchiectasis in both lungs. Also note patchy areas (*arrows*) of mosaic attenuation. (**c**) Coronal reformatted CT image (2.0-mm section thickness) demonstrates extensive bronchiectasis and cellular bronchiolitis of tree-in-bud signs (*arrowheads*) in both lungs. Also note patchy areas (*arrows*) of mosaic attenuation. (**d**) Gross pathologic specimen of explanted right lung discloses bronchiectatic and bronchiolectatic airways filled with abscess (numerous yellow necrotic nodules, *arrows*) down to membranous bronchiolar level. Also note bullae (*open arrow*) in right upper lobe

predispose to sinusitis, recurrent pulmonary infections, and bronchiectasis [39]. Situs inversus totalis or heterotaxy is seen in approximately 50 % of patients. Williams–Campbell syndrome is a congenital form of bronchiectasis usually identified in infancy. It shows familial clustering and may be associated with other congenital abnormalities [40].

ABPA results from both type I and type III hypersensitivity reactions to the endobronchial growth of *Aspergillus* species and is characteristically associated with eosinophilia, symptoms of asthma, and typical imaging findings [8]. It is seen almost exclusively in patients with asthma or cystic fibrosis.

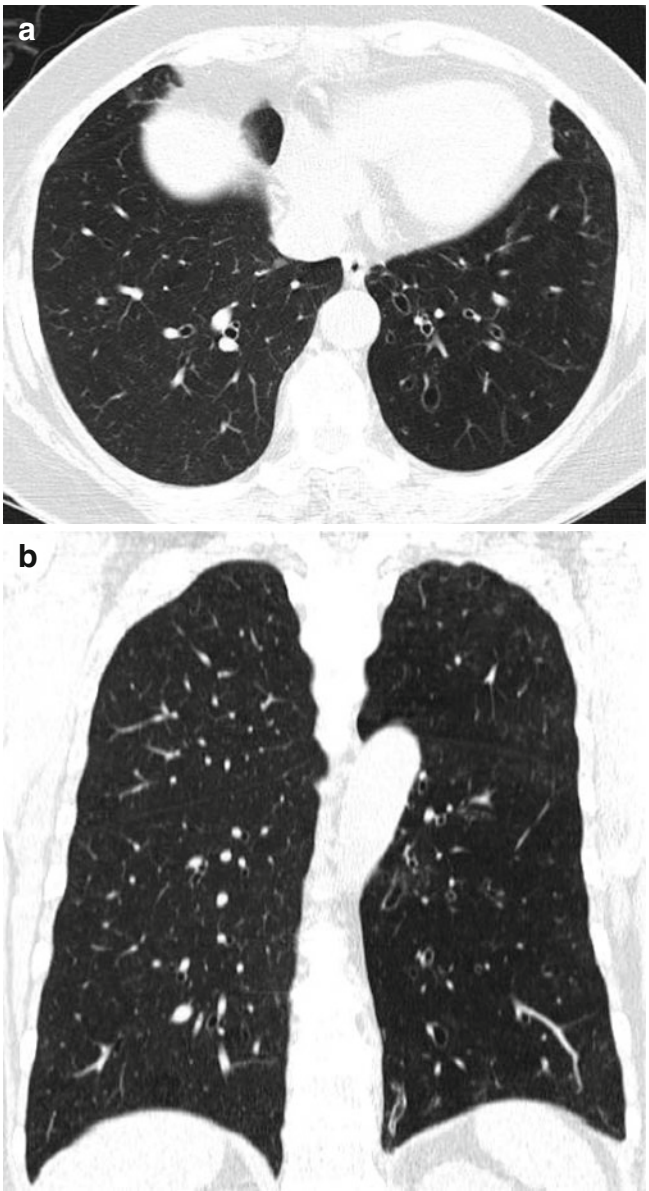

Fig. 13.6 Swyer-James-MacLeod syndrome in a 71-year-old woman. (**a**) Lung window images of CT scans (2.5-mm section thickness) obtained at level of liver dome show bronchiectasis in left lower lobe. Also note mosaic attenuation in bronchiectatic left lower lobe. (**b**) Coronal reformatted image (2.0-mm section thickness) demonstrates bronchiectasis exclusively in left lung. Also note decreased lung attenuation in left lung

Key Points for Differential Diagnosis

1. Reported diagnostic accuracy of HRCT in predicting specific etiologies of bronchiectasis range from 35 to 61 % [41, 42]. In a study, correct diagnosis was reached in 68 % of cases in cystic fibrosis, 67 % of cases in tuberculosis, and 56 % of cases in ABPA [42]. In this study, a bilateral upper lobe distribution was most commonly seen in patients with cystic fibrosis (76 %) and ABPA (56 %), whereas unilateral upper lobe distribution was most common in patients with tuberculosis, and a lower lobe distribution was most often seen in patients after childhood viral infections.
2. HRCT findings of bronchiectasis and bronchiolitis involving more than five lobes, especially when associated with lobular consolidation or a cavity, are highly suggestive of nontuberculous mycobacterial pulmonary disease [43].
3. In addition to bronchiectasis, Swyer-James-MacLeod syndrome is characterized by a hyperlucent lung or lobe, decreased vascularity, and normal or decreased size of the involved lung or lobe on inspiratory images and air trapping on expiratory images [44].
4. Except for Kartagener's syndrome (situs inversus, sinusitis, bronchiectasis), the imaging findings of dyskinetic cilia syndrome are nonspecific.
5. The characteristic HRCT findings of ABPA consist of bronchiectasis and mucoid impaction involving mainly the segmental and subsegmental bronchi of the upper lobes. Although these findings are characteristic features of ABPA, the sensitivity of central bronchiectasis proved to be only 37 % in diagnosing ABPA [37]. In 30 % of patients, the mucoid impaction has high attenuation on CT [45].
6. Characteristic features of traction bronchiectasis are dilatation and beading of the bronchi within areas of fibrosis. In patients with honeycombing, traction bronchiolectasis appears as a cyst on HRCT [46].

Swyer-James-MacLeod Syndrome

Pathology and Pathogenesis

Swyer-James-MacLeod syndrome is a peculiar postinfectious constrictive bronchiolitis that usually affects the lung asymmetrically [47].

Symptoms and Signs

Patients with Swyer-James-MacLeod syndrome frequently have a history of recurrent pulmonary infection and present with nonspecific respiratory symptoms, such as dyspnea on exertion, productive cough, and shortness of breath.

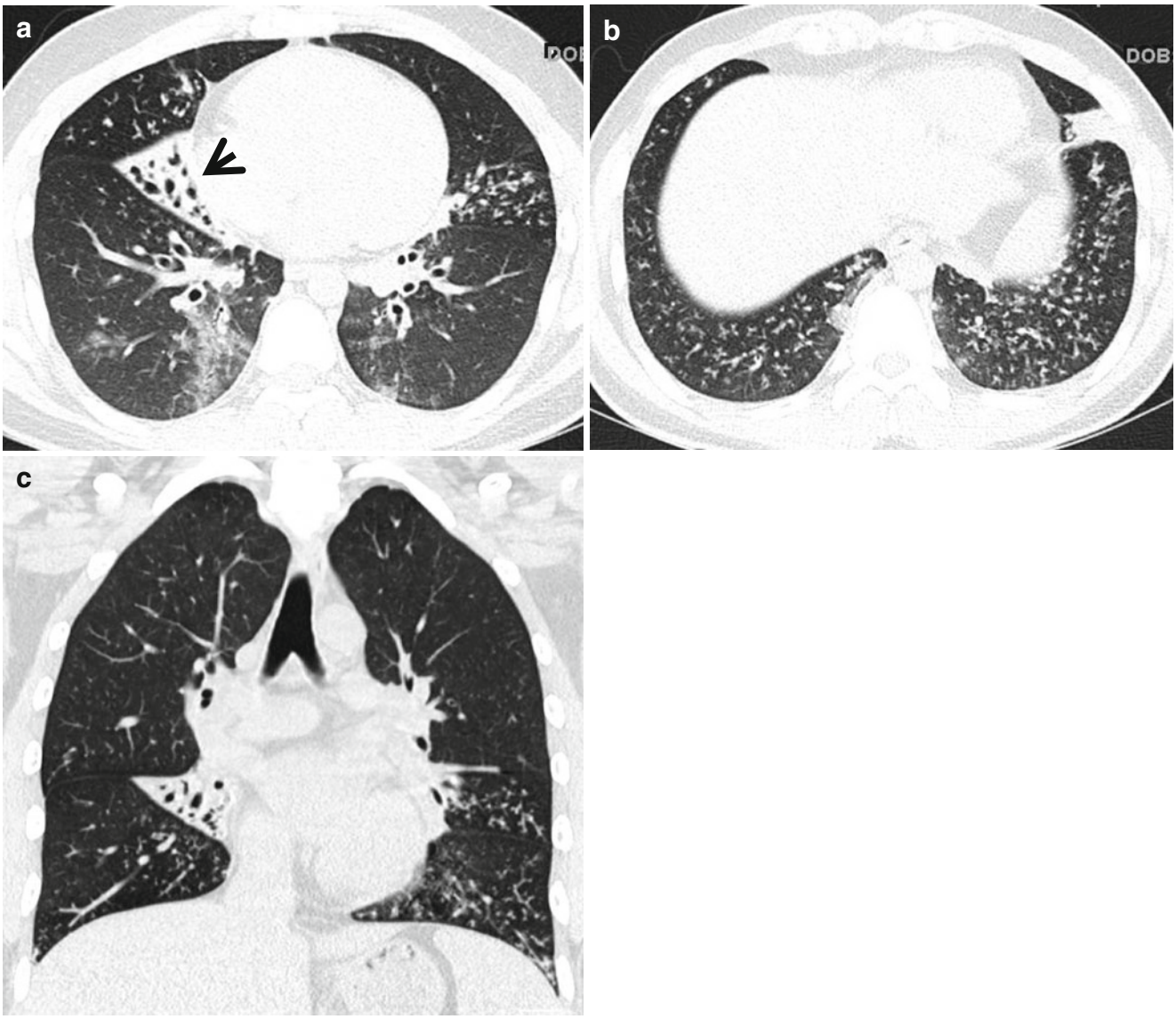

Fig. 13.7 Ciliary dyskinesia syndrome in a 20-year-old man. (**a**, **b**) Lung window images of CT scans (2.5-mm section thickness) obtained at levels of basal segmental bronchi (**a**) and liver dome (**b**), respectively, show extensive bronchiectasis in right middle lobe (*arrow* in **a**), cellular bronchiolitis of tree-in-bud signs in both lungs, and patchy parenchymal opacity areas in both lower lobes. (**c**) Coronal reformatted image (2.0-mm section thickness) demonstrates bronchiectasis exclusively in right middle lobe and cellular bronchiolitis of tree-in-bud pattern in lower lung zones, bilaterally. Abnormal cilia were seen in nasal mucosal examination on electron microscopy (not shown here)

CT Findings

The universal chest CT findings of Swyer-James-MacLeod syndrome are unilateral pulmonary hyperlucency and expiratory air trapping [48]. Bronchiectasis is seen in 60 % of cases (Fig. 13.6) and clinical features and prognosis of patients with Swyer-James-MacLeod syndrome will depend mainly on the presence or absence of saccular bronchiectasis [48]. Other findings include normal- or small-sized lung, lobar collapse, and bronchiectasis. Patchy areas of air trapping in the contralateral lung are also seen.

CT–Pathology Comparisons

In Swyer-James-MacLeod syndrome, unilateral hyperlucency of lung results from decreased pulmonary blood flow secondary to obliterative bronchiolitis.

Patient Prognosis

Unless severe pneumonia is complicated, clinical course of Swyer-James-MacLeod syndrome is relatively good.

Table 13.2 Common diseases manifesting as bronchiectasis or bronchiolectasis

Disease	Key points for differential diagnosis
Bacterial infection	
Staphylococcus, *Klebsiella*	
Mycobacterium tuberculosis	Bronchiectasis usually involves upper lobes
Nontuberculous mycobacterial disease	Bronchiectasis and bronchiolitis involving more than five lobes, especially when associated with lobular consolidation or a cavity
Viral infection	
Swyer-James-MacLeod syndrome	Unilateral pulmonary hyperlucency and expiratory air trapping
HIV infection	
Fungal (histoplasmosis) infection	
Genetic abnormalities	
Cystic fibrosis	Mosaic perfusion, bronchiectasis involving upper lobes
Alpha-1-antitrypsin deficiency	Associated with panacinar emphysema
Dyskinetic cilia syndrome	Central and diffuse bilateral bronchiectasis
Williams–Campbell syndrome	Varicose and cystic bronchiectasis are limited to the fourth-, fifth-, and sixth-generation bronchi
Mounier–Kuhn syndrome	
Immunodeficiency syndromes	
Noninfectious causes	
ABPA	Bronchiectasis involving segmental and subsegmental bronchi of the upper lobes.
Asthma	Thickening and narrowing of the medium-sized and small bronchi, cylindrical bronchiectasis, centrilobular nodules, multifocal and patchy areas of mosaic perfusion
Bronchial obstruction by tumor, foreign body, or congenital abnormalities	
Systemic diseases (collagen vascular disease and inflammatory bowel disease)	

Note: *ABPA* allergic bronchopulmonary aspergillosis

Dyskinetic Cilia Syndrome

Pathology and Pathogenesis

The syndrome has been given its firm pathogenetic basis, when it was recognized that in many cases, the respiratory infections were the consequence of a developmental anomaly consisting of a reduced number of ciliary dynein arms. The term "immotile cilia syndrome" is introduced to encompass all patients with a developmental ciliary defect, regardless of their visceral anatomy, but later the term "primary ciliary dyskinesia" is substituted because the cilia show some movement although they do not beat effectively. The condition is inherited as an autosomal recessive with variable penetrance [49].

Symptoms and Signs

Recurrent upper respiratory tract infection is the main clinical manifestation of early stage of dyskinetic cilia syndrome [50]. When chronic sinusitis and bronchiectasis eventually develop, patients complain of nasal obstruction and chronic production of purulent sputum, with episodes of pneumonia or hemoptysis. Sterility is present in most males due to loss of spermatozoal motility.

CT Findings

The most common CT findings of dyskinetic cilia syndrome include peribronchial thickening, mucus plugging, bronchiectasis, air trapping, ground-glass opacity, or consolidation [51, 52]. Tree-in-bud patterns also may be seen. Pulmonary lesions in patients with dyskinetic cilia syndrome mainly affect the right middle lobe, the lingula, and the lower lobes. Situs inversus (Kartagener's syndrome) is seen in 50 % of patients (Fig. 13.7). Polysplenia and pectus excavatum are associated findings in approximately 8 % of cases.

CT–Pathology Comparisons

The structurally abnormal cilia in dyskinetic cilia syndrome move ineffective and offer a condition predisposing to recurrent pulmonary infection and bronchiectasis.

Patient Prognosis

Although dyskinetic cilia syndrome is not a curable disease, patients with this disorder often have a relatively long life span. Removal of infected secretions from the sinus and bronchial trees and appropriate use of antibiotics is the main therapy for this disorder.

References

1. Hansell DM, Bankier AA, MacMahon H, McLoud TC, Muller NL, Remy J. Fleischner Society: glossary of terms for thoracic imaging. Radiology. 2008;246:697–722.
2. Worthy SA, Muller NL, Hartman TE, Swensen SJ, Padley SP, Hansell DM. Mosaic attenuation pattern on thin-section CT scans of the lung: differentiation among infiltrative lung, airway, and vascular diseases as a cause. Radiology. 1997;205:465–70.
3. Wood BP. Cystic fibrosis: 1997. Radiology. 1997;204:1–10.
4. Lynch DA, Brasch RC, Hardy KA, Webb WR. Pediatric pulmonary disease: assessment with high-resolution ultrafast CT. Radiology. 1990;176:243–8.
5. Grosse C, Grosse A. CT findings in diseases associated with pulmonary hypertension: a current review. Radiographics. 2010;30:1753–77.
6. Small JH, Flower CD, Traill ZC, Gleeson FV. Air-trapping in extrinsic allergic alveolitis on computed tomography. Clin Radiol. 1996;51:684–8.
7. Stern RC. The diagnosis of cystic fibrosis. N Engl J Med. 1997;336:487–91.
8. Jeong YJ, Kim KI, Seo IJ, et al. Eosinophilic lung diseases: a clinical, radiologic, and pathologic overview. Radiographics. 2007;27:617–37; discussion 637–9.
9. King Jr TE. Overview of bronchiolitis. Clin Chest Med. 1993;14:607–10.
10. Hirschmann JV, Pipavath SN, Godwin JD. Hypersensitivity pneumonitis: a historical, clinical, and radiologic review. Radiographics. 2009;29:1921–38.
11. Webb WR. High-resolution computed tomography of obstructive lung disease. Radiol Clin North Am. 1994;32:745–57.
12. Schwickert HC, Schweden F, Schild HH, et al. Pulmonary arteries and lung parenchyma in chronic pulmonary embolism: preoperative and postoperative CT findings. Radiology. 1994;191:351–7.
13. Im JG, Kim SH, Chung MJ, Koo JM, Han MC. Lobular low attenuation of the lung parenchyma on CT: evaluation of forty-eight patients. J Comput Assist Tomogr. 1996;20:756–62.
14. Arakawa H, Webb WR, McCowin M, Katsou G, Lee KN, Seitz RF. Inhomogeneous lung attenuation at thin-section CT: diagnostic value of expiratory scans. Radiology. 1998;206:89–94.
15. Han D, Lee KS, Franquet T, et al. Thrombotic and nonthrombotic pulmonary arterial embolism: spectrum of imaging findings. Radiographics. 2003;23:1521–39.
16. Revel MP, Faivre JB, Remy-Jardin M, Delannoy-Deken V, Duhamel A, Remy J. Pulmonary hypertension: ECG-gated 64-section CT angiographic evaluation of new functional parameters as diagnostic criteria. Radiology. 2009;250:558–66.
17. Sherrick AD, Swensen SJ, Hartman TE. Mosaic pattern of lung attenuation on CT scans: frequency among patients with pulmonary artery hypertension of different causes. AJR Am J Roentgenol. 1997;169:79–82.
18. Brody AS, Klein JS, Molina PL, Quan J, Bean JA, Wilmott RW. High-resolution computed tomography in young patients with cystic fibrosis: distribution of abnormalities and correlation with pulmonary function tests. J Pediatr. 2004;145:32–8.
19. Mogayzel Jr PJ, Naureckas ET, Robinson KA, et al. Cystic fibrosis pulmonary guidelines. Am J Respir Crit Care Med. 2013;187:680–9.
20. Lynch 3rd JP, Weigt SS, DerHovanessian A, Fishbein MC, Gutierrez A, Belperio JA. Obliterative (constrictive) bronchiolitis. Semin Respir Crit Care Med. 2012;33:509–32.
21. Worthy SA, Park CS, Kim JS, Muller NL. Bronchiolitis obliterans after lung transplantation: high-resolution CT findings in 15 patients. AJR Am J Roentgenol. 1997;169:673–7.
22. Leung AN, Fisher K, Valentine V, et al. Bronchiolitis obliterans after lung transplantation: detection using expiratory HRCT. Chest. 1998;113:365–70.
23. Hartman TE, Primack SL, Lee KS, Swensen SJ, Muller NL. CT of bronchial and bronchiolar diseases. Radiographics. 1994;14:991–1003.
24. Padley SP, Adler BD, Hansell DM, Muller NL. Bronchiolitis obliterans: high resolution CT findings and correlation with pulmonary function tests. Clin Radiol. 1993;47:236–40.
25. Klok FA, Mos IC, van Kralingen KW, Vahl JE, Huisman MV. Chronic pulmonary embolism and pulmonary hypertension. Semin Respir Crit Care Med. 2012;33:199–204.
26. Bergin CJ, Rios G, King MA, Belezzuoli E, Luna J, Auger WR. Accuracy of high-resolution CT in identifying chronic pulmonary thromboembolic disease. AJR Am J Roentgenol. 1996;166:1371–7.
27. Remy-Jardin M, Remy J, Louvegny S, Artaud D, Deschildre F, Duhamel A. Airway changes in chronic pulmonary embolism: CT findings in 33 patients. Radiology. 1997;203:355–60.
28. Price LC, Wort SJ, Perros F, et al. Inflammation in pulmonary arterial hypertension. Chest. 2012;141:210–21.
29. McLaughlin VV, Davis M, Cornwell W. Pulmonary arterial hypertension. Curr Probl Cardiol. 2011;36:461–517.
30. Moser KM, Fedullo PF, Finkbeiner WE, Golden J. Do patients with primary pulmonary hypertension develop extensive central thrombi? Circulation. 1995;91:741–5.
31. Humbert M, Sitbon O, Chaouat A, et al. Survival in patients with idiopathic, familial, and anorexigen-associated pulmonary arterial hypertension in the modern management era. Circulation. 2010;122:156–63.
32. Kang EY, Miller RR, Muller NL. Bronchiectasis: comparison of preoperative thin-section CT and pathologic findings in resected specimens. Radiology. 1995;195:649–54.
33. Naidich DP, McCauley DI, Khouri NF, Stitik FP, Siegelman SS. Computed tomography of bronchiectasis. J Comput Assist Tomogr. 1982;6:437–44.
34. Hansell DM. Small airways diseases: detection and insights with computed tomography. Eur Respir J. 2001;17:1294–313.
35. Hogg JC, Macklem PT, Thurlbeck WM. Site and nature of airway obstruction in chronic obstructive lung disease. N Engl J Med. 1968;278:1355–60.
36. Lee KS, Hwang JW, Chung MP, Kim H, Kwon OJ. Utility of CT in the evaluation of pulmonary tuberculosis in patients without AIDS. Chest. 1996;110:977–84.
37. Reiff DB, Wells AU, Carr DH, Cole PJ, Hansell DM. CT findings in bronchiectasis: limited value in distinguishing between idiopathic and specific types. AJR Am J Roentgenol. 1995;165:261–7.
38. Kaneko K, Kudo S, Tashiro M, Kishikawa T, Nakanishi Y, Yamada H. Case report: computed tomography findings in Williams-Campbell syndrome. J Thorac Imaging. 1991;6:11–3.
39. Rosen MJ. Chronic cough due to bronchiectasis: ACCP evidence-based clinical practice guidelines. Chest. 2006;129:122S–31.
40. Lee P, Bush A, Warner JO. Left bronchial isomerism associated with bronchomalacia, presenting with intractable wheeze. Thorax. 1991;46:459–61.

41. Lee PH, Carr DH, Rubens MB, Cole P, Hansell DM. Accuracy of CT in predicting the cause of bronchiectasis. Clin Radiol. 1995;50:839–41.
42. Cartier Y, Kavanagh PV, Johkoh T, Mason AC, Muller NL. Bronchiectasis: accuracy of high-resolution CT in the differentiation of specific diseases. AJR Am J Roentgenol. 1999;173:47–52.
43. Koh WJ, Lee KS, Kwon OJ, Jeong YJ, Kwak SH, Kim TS. Bilateral bronchiectasis and bronchiolitis at thin-section CT: diagnostic implications in nontuberculous mycobacterial pulmonary infection. Radiology. 2005;235:282–8.
44. Moore AD, Godwin JD, Dietrich PA, Verschakelen JA, Henderson Jr WR. Swyer-James syndrome: CT findings in eight patients. AJR Am J Roentgenol. 1992;158:1211–5.
45. Logan PM, Muller NL. High-attenuation mucous plugging in allergic bronchopulmonary aspergillosis. Can Assoc Radiol J. 1996;47:374–7.
46. Nishimura K, Kitaichi M, Izumi T, Nagai S, Kanaoka M, Itoh H. Usual interstitial pneumonia: histologic correlation with high-resolution CT. Radiology. 1992;182:337–42.
47. Kang EY, Woo OH, Shin BK, Yong HS, Oh YW, Kim HK. Bronchiolitis: classification, computed tomographic and histopathologic features, and radiologic approach. J Comput Assist Tomogr. 2009;33:32–41.
48. Lucaya J, Gartner S, Garcia-Pena P, Cobos N, Roca I, Linan S. Spectrum of manifestations of Swyer-James-MacLeod syndrome. J Comput Assist Tomogr. 1998;22:592–7.
49. Storm van's Gravesande K, Omran H. Primary ciliary dyskinesia: clinical presentation, diagnosis and genetics. Ann Med. 2005;37:439–49.
50. Lillington GA. Dyskinetic cilia and Kartagener's syndrome. Bronchiectasis with a twist. Clin Rev Allergy Immunol. 2001;21:65–9.
51. Kennedy MP, Noone PG, Leigh MW, et al. High-resolution CT of patients with primary ciliary dyskinesia. AJR Am J Roentgenol. 2007;188:1232–8.
52. Garcia-Pena P, Boixadera H, Barber I, Toran N, Lucaya J, Enriquez G. Thoracic findings of systemic diseases at high-resolution CT in children. Radiographics. 2011;31:465–82.